NASA

Technical Memorandum 84935

Pair Production in Superstrong Magnetic Fields

J. K. Daugherty and A. K. Harding

FEBRUARY 1983

National Aeronautics and
Space Administration

Goddard Space Flight Center
Greenbelt, Maryland 20771

PAIR PRODUCTION IN SUPERSTRONG MAGNETIC FIELDS

Joseph K. Daugherty

Computer Center

University of North Carolina-Asheville

and

Alice K. Harding

Laboratory for High Energy Astrophysics

NASA/ Goddard Space Flight Center

ABSTRACT

The production of electron-positron pairs by single photons in magnetic fields $\gtrsim 10^{12}$ G has been investigated in detail for photon energies near threshold ($\hbar\omega \gtrsim 2\ mc^2$) as well as for the asymptotic limit of high photon energy. The exact attenuation coefficient, which is derived and then evaluated numerically, is strongly influenced by the discrete energy states of the electron and positron. Near threshold, it exhibits a "sawtooth" pattern as a function of photon energy, and its value is significantly below that predicted by the asymptotic expression for the attenuation coefficient. The energy distributions of the created pair are computed numerically near threshold and analytic expressions are derived in the asymptotic limit. These results indicate that as field strength and photon energy increase, it becomes increasingly probable for the pair to divide the photon energy unequally. This effect, as well as the threshold behavior of the attenuation coefficient, could have important consequences for pulsar models.

I. INTRODUCTION

The possible presence of superstrong magnetic fields ($\gtrsim 10^{12}$ G) around astrophysical objects such as neutron stars has motivated extensive study of the physical processes which can occur in these environments. In particular, quantum-electrodynamical processes such as magnetic pair production and synchrotron radiation in the high field limit have come to play such a central role in pulsar models that a complete understanding of these processes is vital to further theoretical development. In addition, unexplored applications of high magnetic field physics to other objects, e.g. gamma ray burst sources, require further investigation of single photon annihilation and pair production.

The creation of electron-positron pairs by single photons in strong magnetic fields has been studied in a number of instances. The first detailed treatments were carried out independently by Toll (1952) and Klepikov (1954) who calculated the attenuation coefficient for photon pair conversion using the exact Dirac equation for electrons and positrons in a constant, uniform magnetic field, treating the radiation field of the photon as a first order perturbation. Their results, which were in mutual agreement, indicated that even for photon energies well in excess of threshold ($\hbar\omega = 2mc^2$) extremely high magnetic fields ($B > 10^9$ Gauss) were required for a non-negligible rate of pair production. In the limit of high photon energies the rate was found to depend on the parameter $\chi \equiv (\hbar\omega/2mc^2)\,(B \sin\theta/B_{cr})$, where θ is the angle between the field and the photon wave vector, and $B_{cr} = m^2c^3/e\hbar = 4.414 \times 10^{13}$ Gauss. The constant B_{cr} is the critical field strength, in which the gyroenergy $\hbar\omega_c$ of an electron (or positron) is equal to its rest mass.

Since changes in the electron's energy perpendicular to the field occur in quantized increments of $\Delta E \sim \hbar\omega_c$, B_{cr} sets a scale on which to gauge the importance of quantum effects in magnetic fields. The calculated conversion rates indicate that magnetic pair production is not expected to occur with significant probability unless $\chi \gtrsim 0.1$, even though it is kinematically possible for any photon with $\hbar\omega \gtrsim 2mc^2$ to produce a pair, no matter how low χ is.

These results were later reconfirmed and extended by Erber (1966), Baier and Katkov (1968), Rassbach (1971) and Tsai and Erber (1974). These authors were primarily concerned with the derivation of asymptotic expressions for the total pair production rates in the limit of low field strengths ($B \ll B_{cr}$) and photon energies much higher than threshold. However, at energies near threshold, quantum effects due to the discreteness of the electron and positron energies in the magnetic field strongly affect the properties of pair production. When the photon energy and propagation direction are such that $\hbar\omega \sin\Theta \gtrsim 2mc^2$ (a situation which can occur in pulsar cascades) the asymptotic limits become unreliable. Unfortunately, the properties of threshold magnetic pair production have not been sufficiently explored in the published literature and are discussed only qualitatively if at all (Toll 1952). Furthermore, no quantitative treatment of the energy distribution of the created pairs exists, even in the asymptotic limit. Toll (1952) and Arons and Scharlemann (1979) do give qualitative discussions of the differential conversion rates, concluding that the pairs should most probably share the parent photon energy equally, but do not derive expressions for the energy distribution.

This paper is an investigation of these several important areas where gaps exist in the literature on magnetic pair production and which are

relevant to astrophysical applications: properties of pair production near threshold, $\hbar\omega \gtrsim 2mc^2$, and the energy distribution of the pairs, both near threshold and in the asymptotic limit. We also review the previous results with an emphasis on their physical significance and attempt to define more clearly the approximations under which the asymptotic results have been derived. In Section II, we begin with a discussion of the kinematics of pair production which, aside from being of interest in itself, greatly helps to clarify the meaning of the results which follow. The derivation of the exact pair production rate for both photon polarizations is outlined in Section III, in which we also present numerical calculations of the rates and pair energy distributions near threshold. Section IV reviews the derivation of the rate in the asymptotic limit of large photon energy. We also give a comparison of the exact and asymptotic rates and derive the asymptotic pair energy distributions. In Section V, we show how the results can be generalized to arbitrary photon directions and non-vanishing electric fields through Lorentz transformations and discuss in Section VI the importance of some of the new features for models of astrophysical sources.

II. KINEMATICS OF MAGNETIC PAIR PRODUCTION

Consider a photon with energy ω propagating at an angle θ to a uniform magnetic field $\underline{B}$. (Natural units, with $\hbar = c = 1$, will be used throughout). Without loss of generality, it is possible to choose a frame in which $\underline{B} = B\hat{\underline{z}}$, and $\underline{k} = \omega\,(0, \sin\theta, \cos\theta)$. Then the energy-momentum conservation laws governing magnetic pair production may be written as

$$\omega = E_j + E_k \tag{1a}$$

$$\omega \cos\theta = p + q, \tag{1b}$$

where the energy quantum numbers (j, k = 0, 1, 2, ...) and the longitudinal momentum components (p, q) refer to the positron and electron respectively. The Landau energy levels for the two particles have the forms (see for example Johnson & Lippman 1949)

$$E_j = \left[p^2 + m^2\left(1 + 2j\frac{B}{B_{cr}}\right)\right]^{1/2} \tag{2a}$$

$$E_k = \left[q^2 + m^2\left(1 + 2k\frac{B}{B_{cr}}\right)\right]^{1/2} \tag{2b}$$

Note that the conservation laws do not require conservation of momentum perpendicular to the field direction. Indeed, the fact that the external field participates in the particle momentum transfer is what makes this first-order transition kinematically possible. However, it is the "rigidity" of the intense field lines which preserves the energy conservation law [Eqn (1a)].

In the derivation of the photon attenuation coefficients, it is convenient to specialize further to the frame in which $\underline{k}\cdot\underline{B} = 0$, so that $p = -q$. In this frame, equation (1a) may be solved for p to yield

$$p = p(j,k) = \pm m\left[\omega'^2 - 1 - (j+k)B' + (j-k)^2\frac{B'^2}{4\omega'^2}\right]^{1/2} \tag{3}$$

where $\omega' = \omega/2m$, $B' = B/B_{cr}$. Since p^2 must be nonnegative, the allowed transitions to e^+e^- pair states represented by integer pairs (j,k) are just those points in the j-k plane enclosed by the curve $p^2 = 0$, as shown in Figure 1.

It turns out that transitions to states close to this boundary are the most probable, as might be expected from the fact that classically the pair should most probably appear with high "forward" momentum (i.e., large transverse energy levels and relatively small momentum components along the field direction). In any case, the maximum Landau level obtainable by either member of the pair is found by assuming that either j or k = 0 on the boundary curve $p^2(j,k) = 0$, from which it is found that

$$j_{max} = k_{max} \leq \frac{2\omega'(\omega'-1)}{B'}. \qquad (4)$$

For $\omega' \gg 1$, this reduces to $j_{max} \sim \xi \equiv 2\omega'^2/B'$. The parameter ξ appears in the derivation of the attenuation coefficient in Section III below. Similarly, along the symmetry axis j = k, it is found that $j_{max} \leq (\omega'^2 - 1)/2B'$.

The number of integer (j k) pairs enclosed within the boundary $p^2 = 0$ is given approximately by $N_{states}(\omega', B') \sim 2\omega'(\omega' + 2)(\omega' - 1)^2/3B'^2$, which for the limit $\omega' \gg 1$, reduces to $N_{states}(\omega', B') \sim 2\omega'^4/3B'^2$. Hence for fixed B', an increase in the photon energy $d\omega'$ corresponds to an increment $dN_{states} \sim 8\omega'^3 d\omega'/3B'^2$. This number is just twice the number of singularities which appear in the photon attenuation coefficient between energies ω' and $\omega' + d\omega'$, as will be discussed in Section III below.

III. DERIVATION OF THE PHOTON ATTENUATION COEFFICIENT

The S-matrix element for magnetic pair production is simply the first-order transition

$$S_{fi} = ie \int d^4x\, \bar{\psi}_{final}(x)\, \gamma^{\mu} A_{\mu}(x)\, \psi_{initial}(x)$$

where the electron wavefunctions are solutions of the Dirac Hamiltonian for motion in a constant, uniform magnetic field. The precise form of these wavefunctions depends both on the choices of gauge and constants of the motion. The wavefuctions used in the present analysis are described in detail by Daugherty and Bussard (1980); for alternative solutions, see for example Johnson and Lippmann (1949).

The attenuation coefficients for photons whose electric vectors are polarized parallel or perpendicular to the magnetic field direction may be written as

$$R_{\parallel,\perp} = \frac{1}{T} \sum_{j\geq o} \sum_{k\geq o} \int_L \frac{dp}{2\pi} \int_L \frac{dq}{2\pi} \int_L \frac{da}{2\pi\lambda^2} \int_L \frac{db}{2\pi\lambda^2} \left(\sum_{s_+=1}^{2} \sum_{s_-=1}^{2} |S_{fi}|^2_{\parallel,\perp} \right) \qquad (5)$$

where L^3T is the space-time volume element and $\lambda^2 = 1/eB$. The summations over j and k range over all kinematically allowed final states (cf. Fig. 1). The s_- and s_+ summations range over the spin states of the electron and positron. The continuous variables (a,b) are eigenvalues of the x-coordinates of the orbit centers, which are constants of the motion for the wavefunctions used here. As indicated in the earlier discussion on kinematics, the sum over Landau levels j and k is restricted to those states for which $p^2(j,k) \geq 0$ [see equation (3)].

The derivation of the attenuation coefficients using the wavefunctions specified above is straightforward and confirms the results originally obtained by Toll (1952) and Klepikov (1954). For details on techniques for handling the matrix elements, see also Daugherty and Bussard (1980), Appendix I.

The results may be written in the forms

$$R_{\parallel}(\omega',B') = \frac{\alpha_o}{2\xi}\sum_j\sum_k \frac{1}{|p_{jk}|}\{(E_jE_k + m^2 - p^2)(|M(j,k)|^2 + |M(j-1,k-1)|^2)$$

$$+ 2\sqrt{jk}\ B'm^2\ [M^\dagger(j,k)\ M(j-1,k-1) + M^\dagger(j-1,k-1)\ M(j,k)]\} \qquad (6a)$$

$$R_{\perp}(\omega',B') = \frac{\alpha_o}{2\xi}\sum_j\sum_k \frac{1}{|p_{jk}|}\{(E_jE_k + m^2 + p^2)(|M(j-1,k)|^2 + |M(j,k-1)|^2)$$

$$-2\sqrt{jk}\ B'm^2\ [M^\dagger(j-1,k)M(j,k-1) + M^\dagger(j,k-1)M(j-1,k)]\} \qquad (6b)$$

where $\xi = \frac{2\omega'^2}{B'}$,

$$M(j,k) = (-1)^{G-S}\sqrt{\frac{S!}{G!}}\ e^{-\xi/2}\ \xi^{\frac{G-S}{2}}\ L_S^{G-S}(\xi), \qquad (7)$$

and $G = \max(j,k)$, $S = \min(j,k)$..

$L_S^{G-S}(\xi)$ is the generalized Laguerre polymomial, defined according to the standard in Abramowitz & Stegun (1964). These results may also be extended to the cases in which j or k (or both) is zero, if one adopts the convention $L_{-1}^{\alpha}(\xi) \equiv 0$.

The attenuation coefficients are immediately seen to have singularities

or absorption edges whenever ω' and B' have values such that the longitudinal momentum $p(j,k)$ vanishes for any of the allowed transitions (j,k) in the summations of Equation (6). If the attenuation coefficients are considered as functions of ω' for fixed B', these singularities occur at the energies

$$\omega'_{jk} = \tfrac{1}{2}\left(\sqrt{1+2jB'} + \sqrt{1+2kB'}\right) \qquad (8)$$

Figure 2 shows this behavior in the parallel and perpendicular attenuation coefficients in the vicinity of the threshold energy for several field strengths. Two major trends with decreasing field strength to be noted in this figure are the decrease of the typical spacing between peaks and the sharp increase of the attenuation coefficient (averaged over small energy intervals) at energies near threshold. The spacing between peaks can be understood from the kinematical discussion in Section II, and in particular for $\omega' \gg 1$, the number of absorption peaks between ω' and $\omega' + d\omega'$ is approximately

$$dN_{\text{peaks}} = \tfrac{1}{2}\, dN_{\text{states}} \sim \frac{4}{3}\,\frac{\omega'^{3}\, d\omega'}{B'^{2}} \,.$$

The "sawtooth" behavior of the attenuation coefficients has been discussed both by Toll (1952) and Klepikov (1954), but has generally been ignored in astrophysical applications to date. One argument for neglecting such effects is that in pulsar magnetospheres one is typically dealing with energetic photons ($\omega' \gg 1$) and field strengths somewhat less than B_{cr}. Hence one might expect sufficiently small spacing between peaks so that the

well known asymptotic, energy-averaged form of the attenuation coefficients (see Section IV below) are suitable approximations. However, it must be noted that in these same situations, one typically finds that these photons propagate at small angles to the local field direction. Since the asymptotic forms, like the discrete summations [cf. Eqn. (6)] above, apply only to propagation perpendicular to the field, it is in fact necessary to verify (by Lorentz transformations) whether it is still true that $\omega' >> 1$ in the frame for which $\underline{k} \cdot \underline{B} \neq 0$. This question will be pursued in Section V below, where it is shown that typically "energetic" gamma radiation may actually be subject to the near-threshold behavior of the attenuation coefficients.

The relative individual contributions of the (j,k) states in the summations of Equation (6) are illustrated in the plot of Figure 3. As noted earlier, the states nearest the boundary $p^2 = 0$ are by far the most significant. However, Figure 3a suggests that there should be a broad energy distribution for each member of the created pair. This indication is confirmed by the energy distribution obtained by a sampling technique over the (j, k) plane, which is shown in Figure 4. For $B = 10^{12}G$, $\omega = 3$ MeV, there is a strong tendency for the pair to divide the photon energy equally. However, for the case $B = B_{cr}$, $\omega = 3$ MeV, there is actually a greater probability that each member of the pair will be created with an energy near either the minimum ($E = mc^2$) or maximum ($E = \omega - mc^2$) allowable. This behavior near threshold will be compared to energy distributions in two distinct asymptotic regions in Section IV.

IV. ASYMPTOTIC EXPRESSIONS

a) Attenuation Coefficients

For photon energies and field strengths such that the parameter $\xi = 2\omega'^2/B'$ (and hence the number of allowed j-k states for the created pair) becomes large, it is possible to reduce the attenuation coefficients [Eqn (6)] to asymptotic forms which are effectively averaged over small energy intervals to remove the sawtooth behavior. This is feasible because the number of peaks in such small intervals increases rapidly beyond threshold, while the peaks themselves become more narrow at an even faster rate (Toll 1952). The averaging process is actually done by replacing the discrete summations over j,k (in which individual singular contributions make the entire sum infinite) with integrations over continuous variables. Since the contributions from transitions on opposite sides of the symmetry axis j = k in Figures 1 and 3 are identical, it is reasonable to start by defining such variables as follows:

$$u = (j + k)/\xi \tag{9}$$

$$v = (j - k)/\xi$$

In terms of these quantities,

$$p^2 = m^2 \left[\omega'^2(1-2u+v^2)-1\right] \tag{10}$$

Since one integration boundary is determined by the curve $p^2 = 0$, it proves convenient to define a further variable (cf. Figure 1)

$$\phi = (1-2u+v^2)^{1/2} \tag{11}$$

which is then related to p by $p^2 = m^2[\omega'^2\phi^2 - 1]$. The most probable final states lie in the vicinity of $\phi_{min} = 1/\omega'$, hence it will be reasonable to expand quantities in the integrand in powers of ϕ.

The principal ingredient in obtaining these asymptotic results is a suitable approximation for the matrix element M(j,k) defined in Equation (7). A derivation of asymptotic forms for M(j, k) based on that of Klepikov (1954) is given in the Appendix. The reduction of the attenuation coefficients to their asymptotic forms then begins by rewriting the matrix elements M (j, k), M (j-1, k-1), M (j-1, k) and M (j, k-1) entirely in terms of ϕ and v, using Equations (A3), (A6) and (A7). Also, with the use of Equations (9) and (10), the various energy terms in Equation (6) may be expanded to give the following:

$$E_jE_k + m^2 - p^2 \sim m^2[2+\omega'^2(1-v^2-\phi^2)] \tag{12a}$$

$$E_jE_k + m^2 + p^2 \sim m^2\omega'^2(1-v^2+\phi^2) \tag{12b}$$

$$2\sqrt{jk}\,B'\,m^2 \sim m^2\omega'^2\left[1- v^2 - \phi^2\,\frac{(1+v^2)}{(1-v^2)}\right] \tag{12c}$$

The insertion of these expressions and those for the matrix elements into Equation (6), and the replacement of the sums by integrals,

$$\sum_j \sum_k \to 2 \int_{\frac{1}{\omega'}}^{1} d\phi \int_0^{1-\phi} dv\ (2\xi^2\phi)$$

leads to expressions for the (smoothed-out) attenuation coefficients valid for $\xi \to \infty$.

Replacement of the variable ϕ by $\eta = \phi/\phi_{min} = \omega'\phi$ allows the attenuation coefficients to be written in the forms

$$R_{\parallel} \sim \frac{\alpha_o}{\pi} \frac{8}{3\pi^2 \omega'^2 B'} \int_1^\infty d\eta \frac{\eta}{\sqrt{\eta^2-1}} \int_o^1 \frac{dv}{1-v^2}$$

$$\cdot \left\{ \left[\eta^2 + \eta^4 \frac{v^2}{(1-v^2)} \right] K_{1/3}^2(\zeta) + \frac{\eta^4}{1-v^2} K_{2/3}^2(\zeta) \right\} \qquad (13a)$$

$$R_{\perp} \sim \frac{\alpha_o}{\pi} \frac{8}{3\pi^2 \omega'^2 B'} \int_1^\infty d\eta \frac{\eta}{\sqrt{\eta^2-1}} \int_o^1 \frac{dv}{1-v^2}$$

$$\cdot \left\{ \frac{\eta^4}{1-v^2} K_{1/3}^2(\zeta) + \eta^4 \frac{v^2}{(1-v^2)} K_{2/3}^2(\zeta) \right\} \qquad (13b)$$

where $\zeta = \frac{1}{3} \xi \frac{\phi^3}{1-v^2}$.

Klepikov (1954) has written the attenuation coefficient for unpolarized photons in the form

$$\bar{R} = \frac{1}{2}(R_{\parallel} + R_{\perp}) = \frac{\alpha_o}{\pi} B' \frac{2}{3\pi^2 \chi^2} \int_o^\infty dx \int_o^\infty dy \left\{ 2 \cosh^2 y \cosh^5 x \right.$$

$$K_{1/3}^2\left(\frac{2}{3\chi}\cosh^2 y \cosh^3 x\right) - \sinh^2 x \cosh^3 x\, K_{1/3}^2\left(\frac{2}{3\chi}\cosh^2 y \cosh^3 x\right)$$

$$+(2\cosh^2 y - 1)\cosh^5 x\, K_{2/3}^2\left(\frac{2}{3\chi}\cosh^2 y \cosh^3 x\right)\Big\} \qquad (14)$$

where $\chi = \omega' B'$. This expression is found to be equivalent to the average of equations (13a) and (13b) through the replacements

$$\cosh x = \eta$$

$$\cosh y = \frac{1}{\sqrt{1-v^2}} \quad . \qquad (15)$$

In these variables, $\sinh x = (\eta^2 - 1)^{1/2} = p/m$, so that the x integration in Equation (14) is essentially an integration over the longitudinal momentum. The variables v in Equation (13) and y in Equation (14) are related to the energy of the electron or positron through Equations (2), (9), (10) and (11), which give:

$$v = |1 - 2\,\varepsilon|$$

$$1 - v^2 = 4\varepsilon(1 - \varepsilon) \qquad (16)$$

where $\varepsilon = E_j/\omega$ $[E_k/\omega]$ is the fractional energy received by one member of the pair. Therefore, the v and y integrations in Equations (13) and (14) are integrations over the pair energy.

Equations (13) may be further reduced in the limits $\chi \ll 1$ and $\chi \gg 1$.

For the case of small χ in particular, both of the modified Bessel functions approach the asymptotic form

$$K_{1/3}(\zeta) \sim K_{2/3}(\zeta) \sim \left(\frac{\pi}{2\zeta}\right)^{1/2} e^{-\zeta} .$$

Furthermore, the integrand becomes sharply peaked around the symmetry axis (v=0), so that it is permissible to approximate $1/1-v^2$ as $1+v^2$ in the exponential above. Integration over v after this step, followed in turn by the approximation $\eta \sim 1+\rho$, $\rho<<1$, yields the well-known result

$$\bar{R} \sim 0.23 \frac{\alpha_o}{\lambda\!\!\!^{-}} B' \exp\left(-\frac{4}{3\chi}\right). \qquad (17)$$

This is in fact the expression usually assumed in astrophysical calculations, although as shown in Section V below it is sometimes inappropriate. The convergence of the exact attenuation coefficient derived in Section III [cf. Eqn. (6)] to this asymptotic limit is illustrated in Figures 5 and 6. The exact attenuation coefficient is at least several orders of magnitude less than the asymptotic value near threshold for field strengths around 10^{12} Gauss. Below threshold, of course, the asymptotic expression becomes completely invalid.

b) Pair Energy Distributions

The energy distribution of each member of the created pair (which are identical because of the symmetry of the integrand about v = 0) can then be obtained by integrating Equation (13) first over η, and then substituting for v in terms of ε in the resulting integrand. Tsai and Erber (1974) have shown that the polarization-averaged attenuation coefficient [Equation (14)] can be

expressed in a simpler form,

$$\bar{R} \approx \frac{\alpha_o B'}{\chi} \frac{\sqrt{3}}{18\pi\chi} \int_o^1 dv \, \frac{(9 - v^2)}{(1 - v^2)} K_{2/3}[4/3\chi(1 - v^2)] \, . \tag{18}$$

By the simple change of variables of Equation (16) we obtain the differential attenuation coefficient as a function of pair energy:

$$\frac{d\bar{R}(\epsilon,\chi)}{d\epsilon} \approx \frac{\alpha_o B'}{\chi} \frac{\sqrt{3}}{9\pi\chi} \frac{[2 + \epsilon(1-\epsilon)]}{\epsilon(1 - \epsilon)} K_{2/3}\,[1/3\chi\epsilon(1-\epsilon)] \tag{19}$$

which has the asymptotic forms

$$\frac{d\bar{R}\,(\epsilon,\chi)}{d\epsilon} \sim \frac{\alpha_o B'}{\chi} \frac{1}{3\sqrt{2\pi\chi}} \frac{[2 + \epsilon(1-\epsilon)]}{\sqrt{\epsilon(1-\epsilon)}} \exp\,[-1/3\chi\epsilon(1-\epsilon)], \; \chi << 1 \tag{20a}$$

$$\sim \frac{\alpha_o B'}{\chi} \frac{.426}{\pi\chi^{1/3}} \frac{[2 + \epsilon(1-\epsilon)]}{[\epsilon(1-\epsilon)]^{1/3}} \, , \; \chi >> \frac{1}{\epsilon(1-\epsilon)} \tag{20b}$$

These energy distributions have a number of interesting properties. The first to note is that the parameter χ alone determines the shape of the distribution, which has been plotted in Figure 7 for different values of χ using the exact form in Equation (19). For small χ, the distributions are centrally peaked around $\epsilon = 1/2$ and have half-widths $\sim .36\sqrt{\chi}$ for $\chi << 1$. For large χ, the distributions completely change shape, actually becoming peaked at $\epsilon = 0$ and $\epsilon = 1$. For $\chi >> 1$, the shape of the distribution becomes independent of χ altogether. Near $\epsilon = 0$ and $\epsilon = 1$, the condition $\chi >> 1$ does not insure that the argument of $K_{2/3}(x)$ is small, and the exact expression of Equation (19) is needed to describe the drop to zero

at the edges of the distribution. By comparing the curves in Figure 7 to those of Figure 4, it is apparent that the energy distributions near threshold have a similar dependence on χ .

From the behavior of the pair energy distributions, we can conclude that in the case of low fields and photon energies near threshold the pair tend to share the photon energy equally. However, in the case of large fields or high photon energies, there is an increasing tendency for one member of the pair to take all the energy of the photon, while the other receives little more than its rest mass. In the limit $\chi \gg 1$, this is actually the most probable final state of pair production.

V. LORENTZ TRANSFORMATIONS OF THE ATTENUATION COEFFICIENTS

The results of the previous sections all apply to the special Lorentz frame in which $\underline{k}\cdot\underline{B} = 0$. To generalize the (unpolarized) photon attenuation coefficient to frames in which the photon wave vector makes an arbitrary angle θ with the magnetic field, it is sufficient to perform a Lorentz transformation with velocity $v = \cos\theta$ along the field direction. The transformation law for the attenuation coefficient is most easily understood in terms of its inverse, the mean free path, which obeys the simple invariance law

$$\lambda_o^2 - t_o^2 = \lambda^2 - t^2 \tag{21}$$

From this law and the transformation properties of ω and B, it is immediately possible to write

$$\bar{R}\ (\omega,\ \underline{B}) = \sin\theta\ \bar{R}_o(\omega \sin\theta,\ \underline{B}) \qquad (22)$$

where $\bar{R}_o$ is now used to denote the functional form of the attenuation coefficient in the special frame for which $\underline{k}\cdot\underline{B} = 0$, as derived in previous sections. Note that this transformation law is valid for both the exact forms in Eqn (6) and the asymptotic limits of Section IV.

In particular, for the asymptotic case $\chi >> 1$, the well-known approximation [Equation (17)] for the attenuation coefficient appears to be modified simply by the replacement of B with B sin θ. However, from Equation (22) it may be seen that it is really ω which becomes ω sin θ in the product $\chi = (\omega/2m)(B/B_{cr})$. This distinction is quite important, since in the non-asymptotic case the attenuation coefficient does not depend only on χ.

The behavior of the transformed coefficient near threshold is illustrated in Figure 8. Note that the threshold energy itself is displaced upward by the factor 1 / sin θ, which also is the factor by which the energy scale is stretched in the new frame. The reduction of the attenuation coefficients by the factor sin θ is also evident.

The transformation property implies an additional point of interest in pulsar cascade theory. Here a primary electron with energy γmc^2, accelerated along a curved field line, may emit gamma radiation nearly along its direction of motion, within a forward cone of half-angle $\theta \sim 1/\gamma$. To follow such a photon along its trajectory outward through the magnetosphere, it is necessary to perform a sequence of Lorentz transformations at small intervals, where the field makes a slowly increasing angle with the photon wave vector. As Figure 8 illustrates, this sequence of transformations may initially put even high-energy photons below the threshold for pair production, and in such cases these photons will propagate at least until they exceed the local threshold

energy. Hence the near-threshold forms of the attenuation coefficients must be used over some portion of the photon trajectory, and the commonly used asymptotic form may not be appropriate over any portion of the actual photon trajectory before its annihilation.

It may also be noted that a Lorentz transformation in which $\underline{v}$ is perpendicular to $\underline{B}$ may also be used to generalize the attenuation coefficient to situations in which both electric and magnetic fields are present, at least within the restrictions $\underline{B}^2 - \underline{E}^2 > 0$, $\underline{B} \cdot \underline{E} = 0$ (Daugherty and Lerche 1975). Such cases are important for tracing cascades in rapidly rotating pulsars (as for example the Crab pulsar) in which significant rotation-induced electric fields are expected. Here the transformation law for the attenuation coefficients may be written in the form

$$\bar{R}(\omega, \underline{B}) = \gamma(1 - \eta_x v)\, \bar{R}_o(\gamma\omega(1-\eta_x v), \frac{B}{\gamma}) \tag{23}$$

in which (η_x, η_y, η_z) are the photon direction cosines in a frame chosen so that $\underline{B} = B\,\hat{z}$, $\underline{E} = E\,\hat{y}$, the velocity of transformation $\underline{v} = \underline{E}\times\underline{B}/B^2$, and the Lorentz factor $\gamma = (1 - E^2/B^2)^{-1/2}$.

The full generalization to situations in which electric fields both parallel and perpendicular to $\underline{B}$ are present requires explicit calculation of the attenuation coefficients using the Schwinger proper-time technique (Urrutia 1978). However, for known pulsars the ratio $E_\parallel/B$ is sufficiently small that such cases are of only minor interest in cascade theory (Ayasli 1978, Harding et al. 1978).

VI. DISCUSSION

We have obtained results on several aspects of magnetic pair production which should be of interest in future astrophysical applications. The pair production attenuation coefficient near threshold is dominated by magnetic field quantum effects, showing sharp resonance peaks at photon energies corresponding to discrete states of the electron and positron. As the field approaches the critical field strength, the spacing of these peaks at threshold increases, approaching $mc^2/\sin\theta$. As the photon energy increases above threshold at a given magnetic field strength, the peak spacings decrease rapidly and the mean value of the attenuation coefficient approaches, from below, the asymptotic limit derived for very large pair quantum numbers. The parameter $\xi \equiv 2\omega'^2/B'$, which is the number of the highest energetically allowed Landau state available to either the electron or positron, is <u>not</u> a Lorentz invariant quantity and must be evaluated in the frame in which the photon propagates perpendicular to the field. Thus, the asymptotic condition $\xi \gg 1$ does not ensure that threshold (quantum) effects are unimportant in an arbitrary frame. Neither is the threshold energy for pair production frame invariant; in an arbitrary frame in which the photon propagates at an angle θ to the field, the threshold energy is $2mc^2/\sin\theta$. This result has the somewhat surprising consequence that even extremely high energy photons, if they are propagating at very small angles to the field, may have perpendicular energies below threshold.

Since the complicated expressions [cf. Eqn (6)] for the threshold attenuation coefficients are unwieldy for practical calculations involving pair production, we give here an analytic expression which approximates their average behavior, and also describes their approach to the asymptotic limit. For $\chi < 1$,

$$\bar{R} \approx 0.23 \frac{\alpha}{\chi} B' \exp\left[-\frac{4 f(\omega', B')}{3\chi}\right] \qquad \omega' \geq 1,$$

$$0 \qquad \omega' < 1,$$

$$\text{where } f(\omega', B') = 1 + 0.42\, \omega'^{-2.7} - .0038\, B' \qquad (24)$$

The function $f(\omega', B')$ has been obtained by a three parameter fit to the attenuation coefficient $\bar{R}(\omega', B')$ averaged over fixed intervals of ω' large enough to contain at least several resonance peaks. The fit is not terribly sensitive to the B' dependence, owing to uncertainties from averaging over the the peaks. We point out that the threshold condition, $\omega' \geq 1$, must be put in artifically, and that the expression for arbitrary photon angles may be obtained using eqn (22). It is interesting tc note that while the asymptotic expression [Eqn (17)] is a function only of χ, the exact attenuation coefficient, as approximated by Eqn (24), depends on ω' and B' independently.

We have also found that the probability distribution of pair energies is determined by the parameter χ, which is Lorentz invariant (for the case of a pure B field and transformations along B). For small χ, the most probable pair energy is half of the parent photon energy. In the limit of large χ, the most probable final state is one where the photon energy is given almost entirely to one member of the pair. This unequal division of the photon energy was shown by Sokolov et. al. (1974) to be the case for $B \gtrsim B_{cr}$ where, of course, χ is always greater than 1. From the results derived in Section IV, however, we have shown that unequal divis:on of the photon energy can occur also for $B < B_{cr}$, as long as $\chi > 1$. Probability distributions of pair energy very similar to those of Figure 7 have been computed for both γ-γ pair production (Burns and Lovelace 1982; Burns, private communication) and γ-nucleus pair production (Rossi and Greisen 1941) which also are seen to change their shape as a function of a single parameter characterizing each process.

The production of pairs with one member of the pair receiving all the photon energy, and therefore occupying a high Landau state, while the other member receives only its rest mass, thus occupying the ground state, is possibly related to the dominance of ground state transitions in synchrotron radiation. It has been found (Sokolov et al. 1973; White 1974, 1976) that transitions of an electron from an excited state to the ground state in a magnetic field become more probable as the field approaches and exceeds the critical field strength. This tendency of the electron to radiate away all its energy via a single photon causes the tail of the synchrotron spectrum to rise near the "tip", where $\hbar\omega$ equals the electron energy. Although the kinematics of this process are different from those of pair production, the probability distribution of initial and final states of synchrotron radiating electrons in a near critical field would look very similar to the pair distributions we have found for $\chi \gg 1$.

The properties of magnetic pair production explored in this paper have immediate significance for pulsar models. In current polar cap models (eg. Ruderman and Sutherland 1975, Arons and Scharlemann 1979), particles are accelerated to high energies (10^{12}-10^{13} eV) along magnetic field lines and emit γ-ray photons through curvature radiation. These photons are initially propagating parallel to the field and thus have $\omega \sin\theta = 0$. In order to produce pairs, they must acquire a $\sin\theta$ large enough to (at least) reach threshold by traveling a straight trajectory in the curved and rotating dipole field. If $B \gtrsim 10^{12}$ G, these photons will have $\omega \sin\theta \sim 2mc^2$ when they pair produce and the asymptotic attenuation coefficient will under-estimate their mean free paths because (1) it overestimates the exact attenuation coefficient near threshold and (2) it has a non-zero (and possibly large) value below threshold. The absorption of photons in strong fields may be further complicated by threshold

behavior of the vacuum index of refraction. Shabad and Usov (1982) have argued that curvature photons in fields $> 5 \times 10^{12}$ G will be refracted along the direction of B. If this is the case, then the photon mean free paths will be even larger. In any event, the increase in mean free paths from the pair production threshold behavior may be regarded as a lower limit.

Since the e^+e^- pairs produced within the accelerating region tend to short out the electric field, the spatial extent of this region is proportional to the photon mean free path. Larger mean free paths will increase the distance over which the voltage drop occurs. However, due to the weak dependence of the size of the voltage drop on the altitude at which the shorting-out occurs in these models, the acceleration energies may not be much larger.

The increased mean free paths are expected to have a larger effect on the cascades which occur above the accelerating region. Threshold effects on individual mean free paths will be magnified by the numbers of photons involved and could produce significant changes in the predicted γ-ray and pair spectra for fields in excess of $\sim 4 \times 10^{12}$ G. Use of the computed pair energy distributions in simulations of pulsar cascades may also have interesting effects. Most previous calculations of this sort (Daugherty and Harding 1982, Ogelman et al. 1976) have assumed that the pairs are always produced with one-half the parent photon energy. As we have shown here, the energy distributions are in fact quite broad for $\chi \gtrsim 0.1$ when pair production is most likely to occur. Both of these topics will be the subject of future investigation.

We thank T. Erber, F. C. Jones and M. L. Burns for helpful conversations and comments and J. Arons for his suggestions as referee. We are also

grateful to M. McMullen and A. Szymkowiak for programming assistance. J. K. D. was supported in part by a grant from the NASA/ASEE Summer Faculty Fellowship Program and also by the Research Corporation.

APPENDIX

Derivation of Asymptotic Forms for M(j,k)

Following Klepikov (1954), we start from the contour integral representation for the generalized Laguerre polynomial

$$L_S^{G-S}(\xi) = \frac{1}{2\pi i} \int \frac{dz}{z} e^{\xi z} \frac{(1-z)^G}{(-z)^S}, \qquad (A1)$$

where the contour encloses the origin. Replacement of G and S by the parametized variables defined in Equations (9) and (11) above allows one to write the saddle points of the integrand as

$$z_\pm = 1/2 \ (1 - \nu \pm \phi) \qquad (A2)$$

Both of these points lie on the positive real axis, and the inner point z_- may be crossed by initially deforming the original contour about the origin.

However, such a straightforward application of the method of steepest descents proves insufficient when $\phi \to \phi_{min} = 1/\omega'$, for then the two saddle points (which are oriented in mutually perpendicular fashion) move quite close together. Hence the precise choice of contour through the point z_- is critical. Klepikov's approach is to make the transformation $z = z_- e^t$ and then to expand the resulting exponential function of t about the origin (which

is now also the saddle point), retaining powers up to t^3. This method yields an approximation for the Laguerre polynomials which, when combined with Stirling's approximation for the factorial functions in Equation (7), yields finally

$$|M(j,k)| + |M(\phi,v)| \sim \frac{1}{\sqrt{3\pi}} \frac{\phi}{\sqrt{1-v^2}} K_{1/3}(\zeta) \qquad \text{(A3)}$$

where

$$\zeta = \frac{1}{3} F \frac{\phi^3}{1-v^2} \qquad \text{(A4)}$$

An unfortunate complication which arises in the expressions in Equation (6) for the attenuation coefficients is that the quantities M(j-1, k-1), M(j-1,k) and M(j,k-1) all appear in addition to M(j,k). While in the limits of large (j, k) these adjacent matrix elements approach M(j,k) itself, the small remaining differences must be taken into account in Equation (6). The principal reason is that each coefficient is found to be the difference of two terms which are nearly identical, so that the small differences in the matrix elements in distinct terms are significant in the final result. The technique for finding the adjacent matrix elements involves the use of the relations

$$x \frac{dL_n^{\alpha}(x)}{dx} = nL_n^{\alpha}(x) - (n+\alpha)L_{n-1}^{\alpha}(x) \qquad \text{(A5a)}$$

$$\frac{dL_n^{\alpha}(x)}{dx} = -L_{n-1}^{\alpha+1}(x) \qquad \text{(A5b)}$$

$$L_n^{\alpha-1}(x) = L_n^{\alpha}(x) - L_{n-1}^{\alpha}(x) \tag{A5c}$$

for the generalized Laguerre polynomials to prove the following relations between the matrix elements:

$$\sqrt{jk}\, M(j-1,k-1) = \frac{1}{2}(j+k-\xi)\, M(j,k) - \xi \frac{dM(j,k)}{d\xi} \tag{A6a}$$

$$i\sqrt{j\xi}\, M(j-1,k) = -\left(\frac{\xi-k+j}{2}\right)M(j,k) - \xi \frac{dM(j,k)}{d\xi} \tag{A6b}$$

$$-i\sqrt{k\xi}\, M(j,k-1) = \left(\frac{\xi+k-j}{2}\right)M(j,k) + \xi \frac{dM(j,k)}{d\xi} \tag{A6c}$$

From Equation (A3) it is found that

$$\frac{dM(j,k)}{d\xi} \sim \frac{-1}{2\sqrt{3\pi}} \frac{\phi^2}{\sqrt{1-v^2}} K_{2/3}(\zeta) \tag{A7}$$

Substitution of Equations (A7) and (A3) into (A6) then gives expressions for the adjacent matrix elements in terms of ϕ and v.

REFERENCES

Abramowitz, M. and Stegun, I. A. (ed.) 1964, "Handbook of Mathematical Functions" (National Bureau of Standards).

Arons, J. and Scharlemann, E. T. 1979, Ap. J., 231, 854.

Ayasli, S. 1978, Ph.D. thesis, Middle East Tech. Univ., Ankara, Turkey.

Baier, V. N. and Katkov, V. M. 1968, Soviet Phys. JETP, 26, 854.

Burns, M. L. and Lovelace, R. V. E. 1982, Ap.J., in press.

Cheng, A. F. and Ruderman, M. A. 1977, Ap. J., 214, 598.

Daugherty, J. K. and Bussard, R. W. 1980, Ap. J., 238, 296.

Daugherty, J. K. and Harding, A. K. 1982, Ap. J., 252, 337.

Daugherty, J. K. and Lerche, I. 1975, Ap. Space Sci., 38, 437.

Erber, T. 1966, Rev. Mod. Phys., 38, 636.

Harding, A. K., Tademaru, E. and Esposito, L. W. 1978, Ap. J., 225, 226.

Johnson, M. H. and Lippmann, B. A. 1949, Phys. Rev., 76, 828.

Klepikov, N. P. 1954, Zh. Eksp. Teor. Fiz., 26, 19.

Ogelman, H., Ayasli, S. and Hacinliyan, A. 1976, "The Structure and Content of the Galaxy and Galactic Gamma Rays" ed. C. E. Fichtel and F. W. Stecker (NASA, Washington, D. C.).

Rassbach, M. E. 1971, Ph.D. Thesis, Caltech.

Rossi, B. and Greisen, K. 1941, Rev. Mod. Phys., 13, 240.

Ruderman, M. A. and Sutherland, P. G. 1975, Ap. J., 196, 51.

Shabad, A. E. and Usov, V. V. 1982, Nature, 295, 215.

Sokolov, A. A., Zhukovskii, V. Ch. and Nikitina, N. S. 1973, Phys. Lett., 43A, 85.

Sokolov, A. A., Ternov, I. M., Borison, A. V. and Zhukovskii, V. Ch. 1974, Phys. Lett., 49A, 9.

Toll, J. S. 1952, Ph.D. Thesis, Princeton University.

Tsai, W. and Erber, T. 1974, Phys. Rev. D, 10, 492.

Urrutia, L. F. 1978, Phys. Rev. D, 17, 1977.

White, D. 1974, Phys. Rev. D, 9, 868,

White, D. 1976, Phys. Rev. D, 13, 1791.

FIGURE CAPTIONS

Figure 1: Kinematically allowed Landau states for the created electron-positron pair with principal quantum numbers (j, k), for the case $B = B_{cr}$, $\omega = 3$ MeV. These states are determined by the condition $p^2 > 0$ [cf. Equation (3)] which, as illustrated, is the area inside the line $p = 0$. The variables v and ϕ are used in the derivation of the asymptotic limit in Section IV [cf. Equation (9)].

Figure 2: Exact attenuation coefficient for pair production [cf. Equation (6)] in the case where the photon propagates perpendicular to a pure magnetic field, plotted against photon energy. Threshold energy is 1.022 MeV, below which $R(\omega) = 0$.

a) Attenuation coefficients for polarization (of the electric vector) parallel and perpendicular to a magnetic field at the critical field strength.

b) Attenuation coefficient averaged over both polarizations for $B = 5 \times 10^{12}$G.

Figure 3: Relative contributions of individual (j, k) states of the created electron-positron pair to the total pair production attenuation coefficient for the cases

a) $B = B_{cr} = 4.414 \times 10^{13}$G, $\omega = 3$ MeV, having $j_{max} = 11$ and

b) $B = 10^{12}$G, $\omega = 3$ MeV, having $j_{max} = 502$

The vertical scales are log scales with an artificial lower cutoff.

Figure 4: Energy distribution of one member of the created pair, computed from an integration over the (j,k) probability distributions of Figure 3. Plotted here is the normalized probability density as a function of pair energy E divided by photon energy ω. Any asymmetries in the distributions about $E/\omega = 0.5$ are due to statisitcal errors in the Monte Carlo sampling used.

Figure 5: Comparison of the exact and asymptotic pair production attenuation coefficients, $\bar{R}$ and $\bar{R}_A$, averaged over both photon polarizations, for two field strengths. Each "X" point for $B = 10^{12}$G is an average of the exact attenuation coefficient over the many absorption edges (which are much more closely spaced then the absorption edges for $B = 5 \times 10^{12}$G) in the surrounding energy interval.

Figure 6: Convergence of the exact attenuation coefficient to its asymptotic limit for a field of 10^{12}G. The ratio of the asymptotic to the exact attenuation coefficient, as shown in Figure 5, are plotted against photon energy. Dependence on the parameters χ and ξ (see text) is also shown.

Figure 7: Energy distribution of one member of the electron-positron pair, derived in the asymptotic limit [cf. Equation (19)] for different values of $\chi = (\hbar\omega/2mc^2)\ (B/B_{cr})$. The quantities plotted here are the same as those of FiG. 4.

Figure 8: Lorentz-transformed pair production attenuation coefficient for

the case $\sin\theta = 0.2$, where θ is the angle between the magnetic field and the photon propagation vector.

JOSEPH K. DAUGHERTY: Computer Center, University of North Carolina, Asheville, NC 28804.

ALICE K. HARDING: Code 665, NASA Goddard Space Flight Center, Greenbelt, MD 20771.

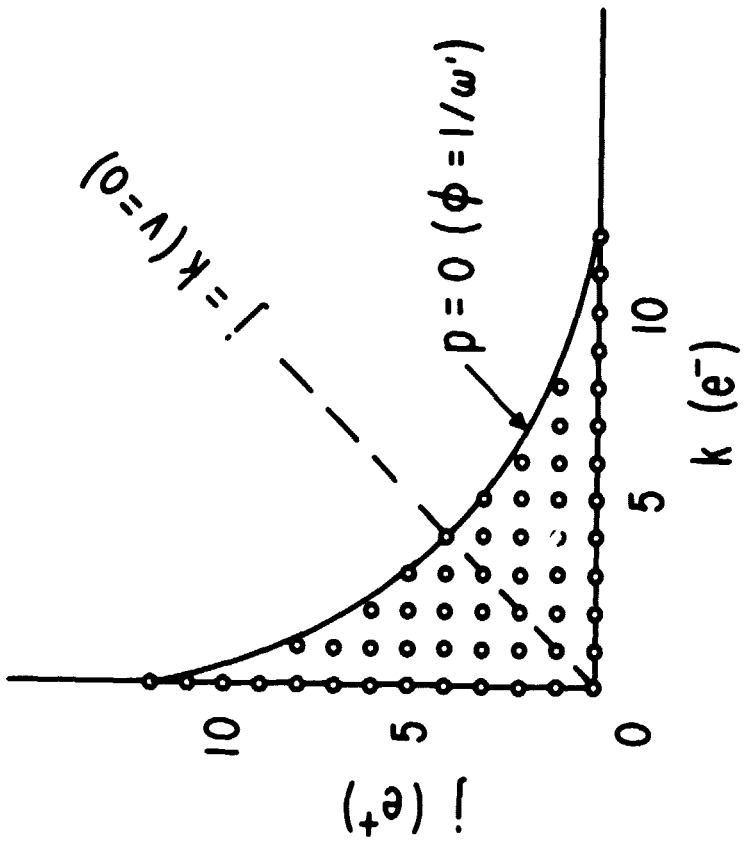

Figure 1

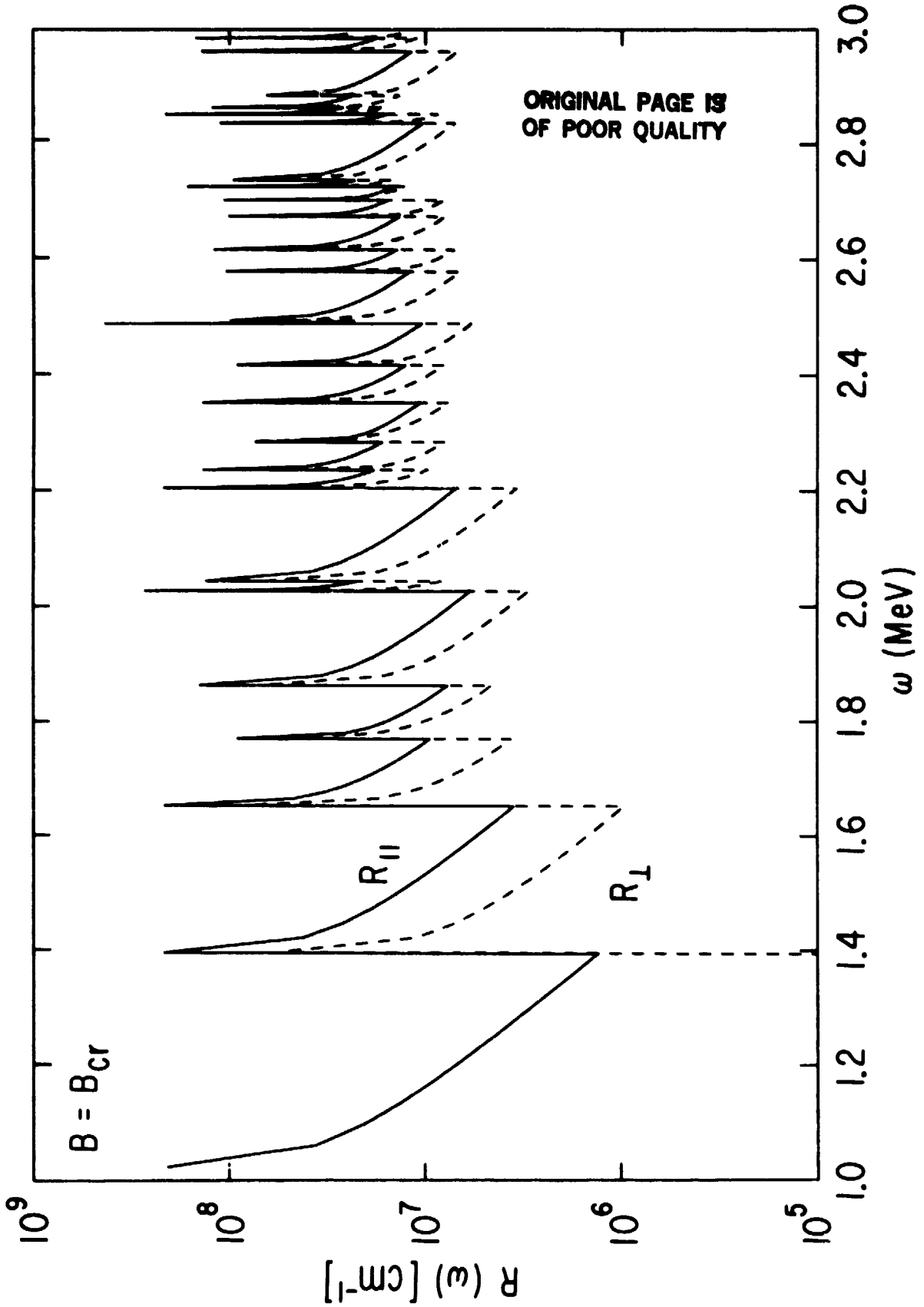
ORIGINAL PAGE IS
OF POOR QUALITY
B = B_cr
R_II
R_⊥
R (ω) [CM⁻¹]
ω (MeV)
10⁹
10⁸
10⁷
10⁶
10⁵
1.0
1.2
1.4
1.6
1.8
2.0
2.2
2.4
2.6
2.8
3.0

Figure 2a

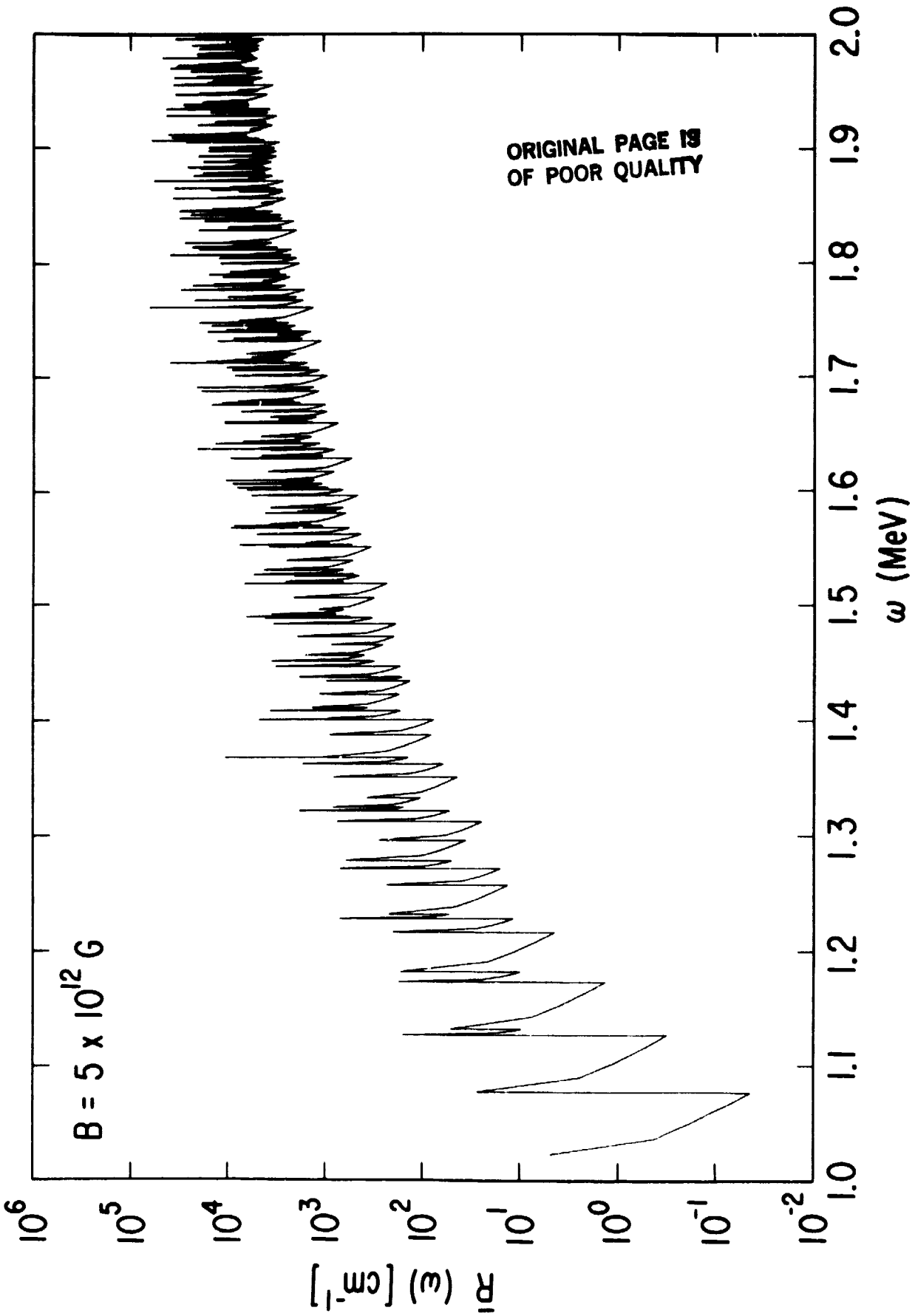
ORIGINAL PAGE IS
OF POOR QUALITY
B = 5 x 10^12 G
R (ω) [cm^-1]
ω (MeV)
10^6
10^5
10^4
10^3
10^2
10^1
10^0
10^-1
10^-2
1.0
1.1
1.2
1.3
1.4
1.5
1.6
1.7
1.8
1.9
2.0

Figure 2b

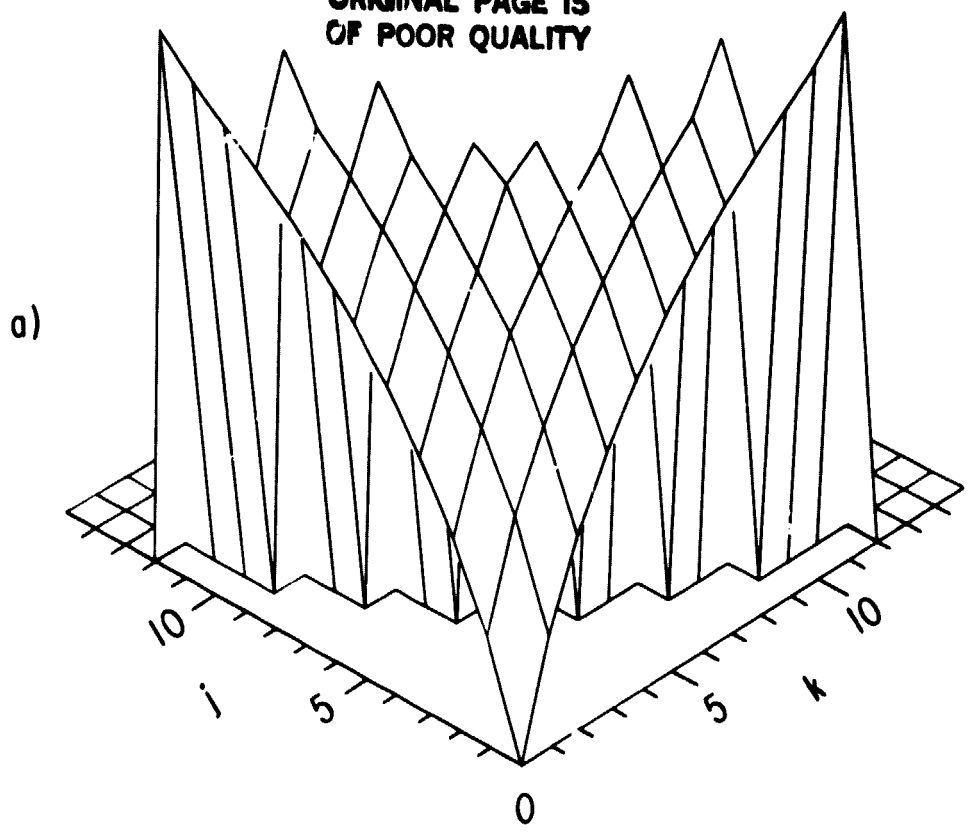

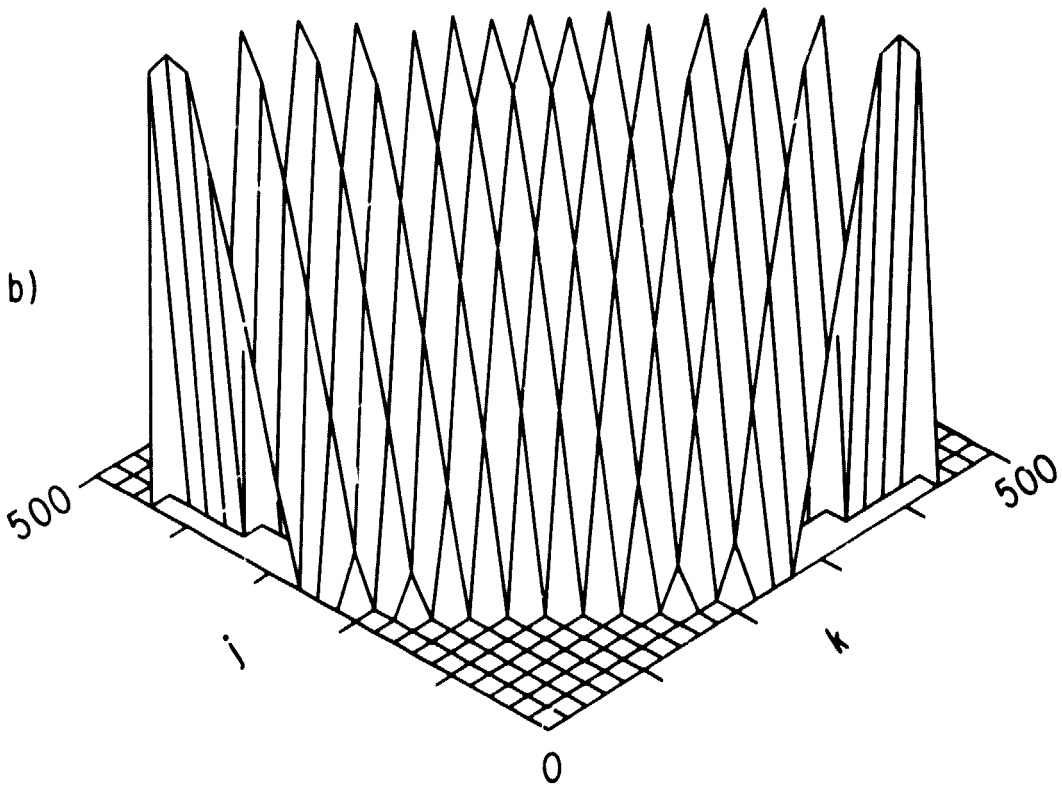

Figure 3

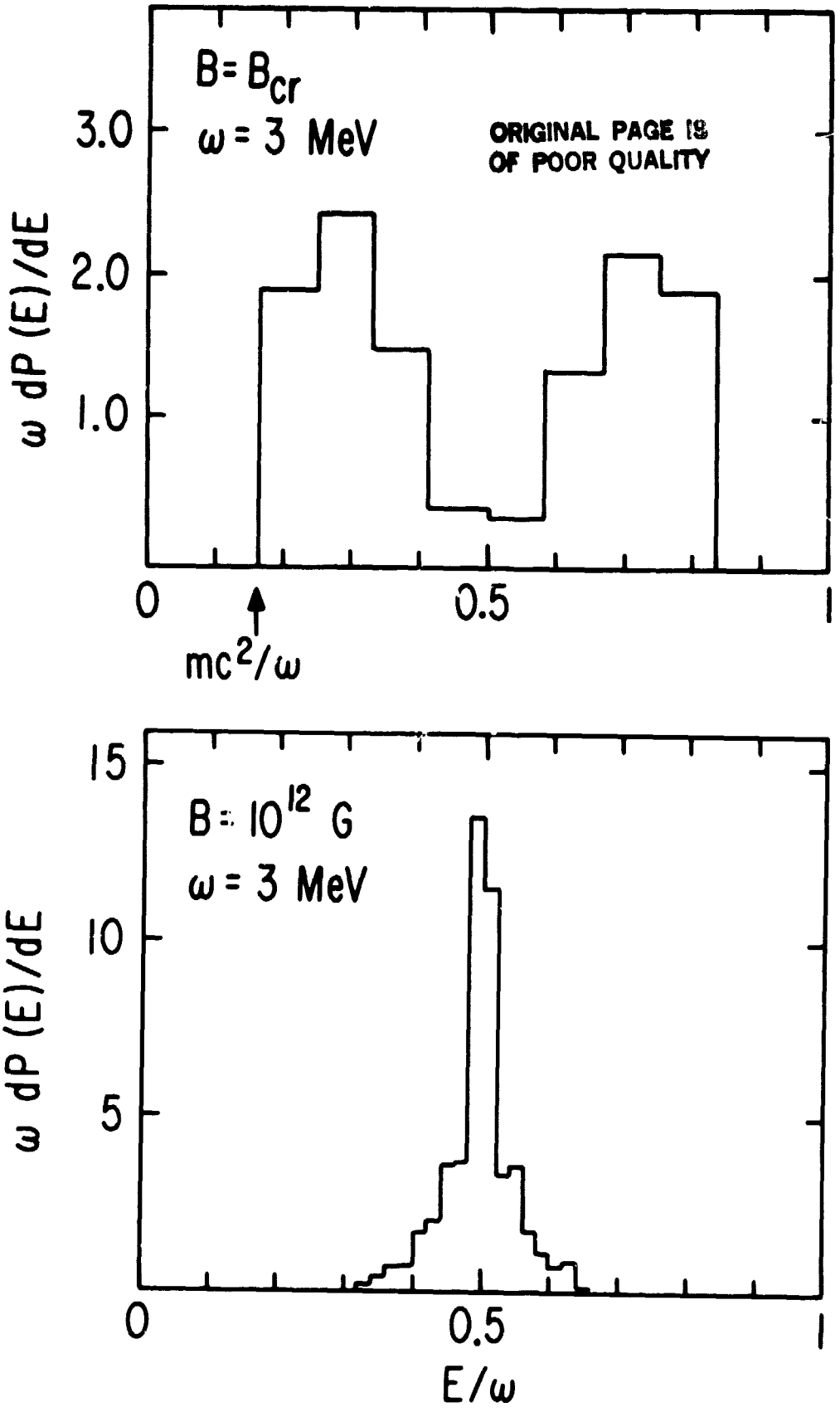
B= B_cr
ω = 3 MeV
ORIGINAL PAGE IS
OF POOR QUALITY
3.0
2.0
1.0
ω dP (E)/dE
0
0.5
1
mc²/ω
B = 10¹² G
ω = 3 MeV
15
10
5
ω dP (E)/dE
0
0.5
1
E/ω

Figure 4

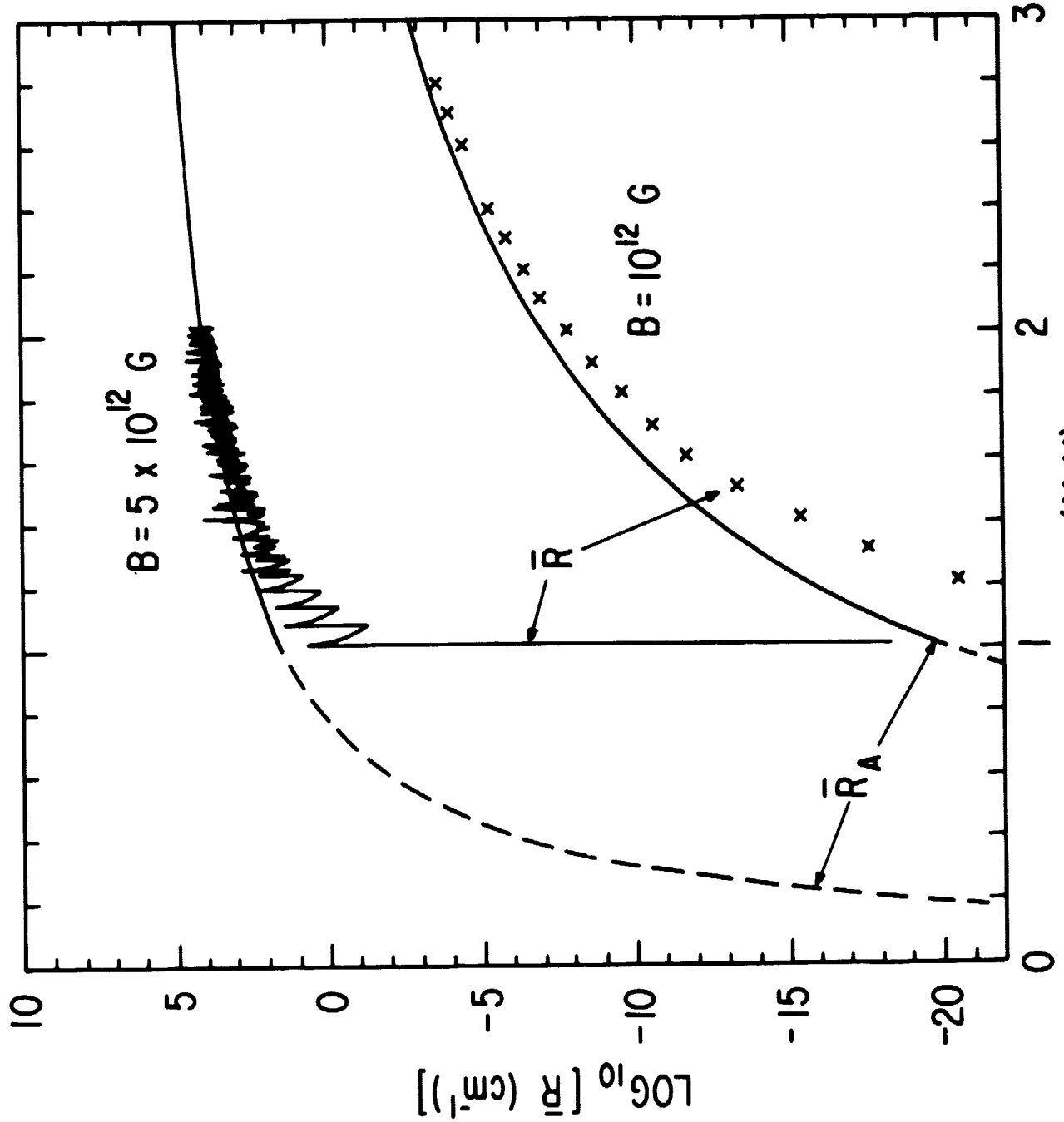

Figure 5

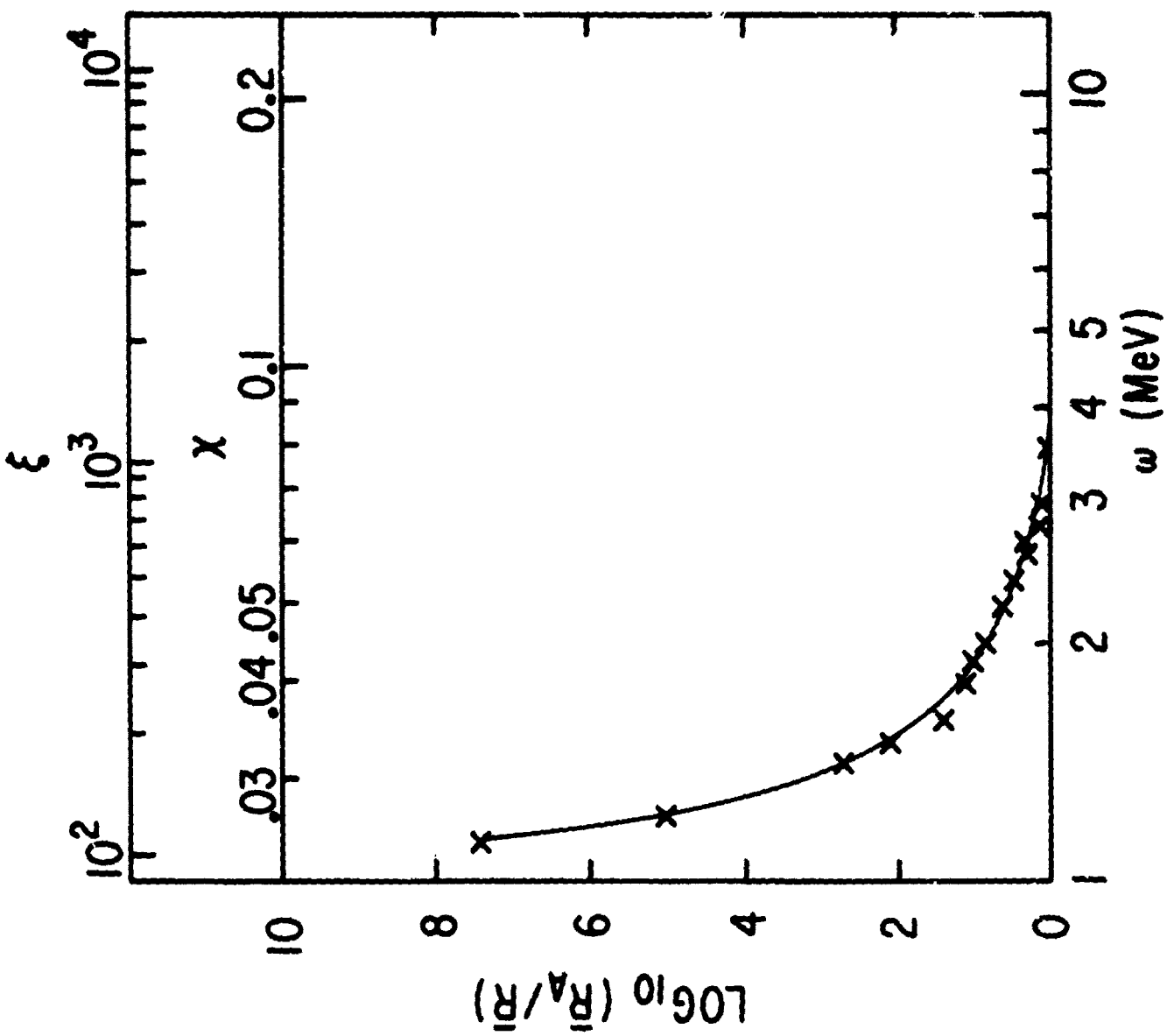

Figure 6

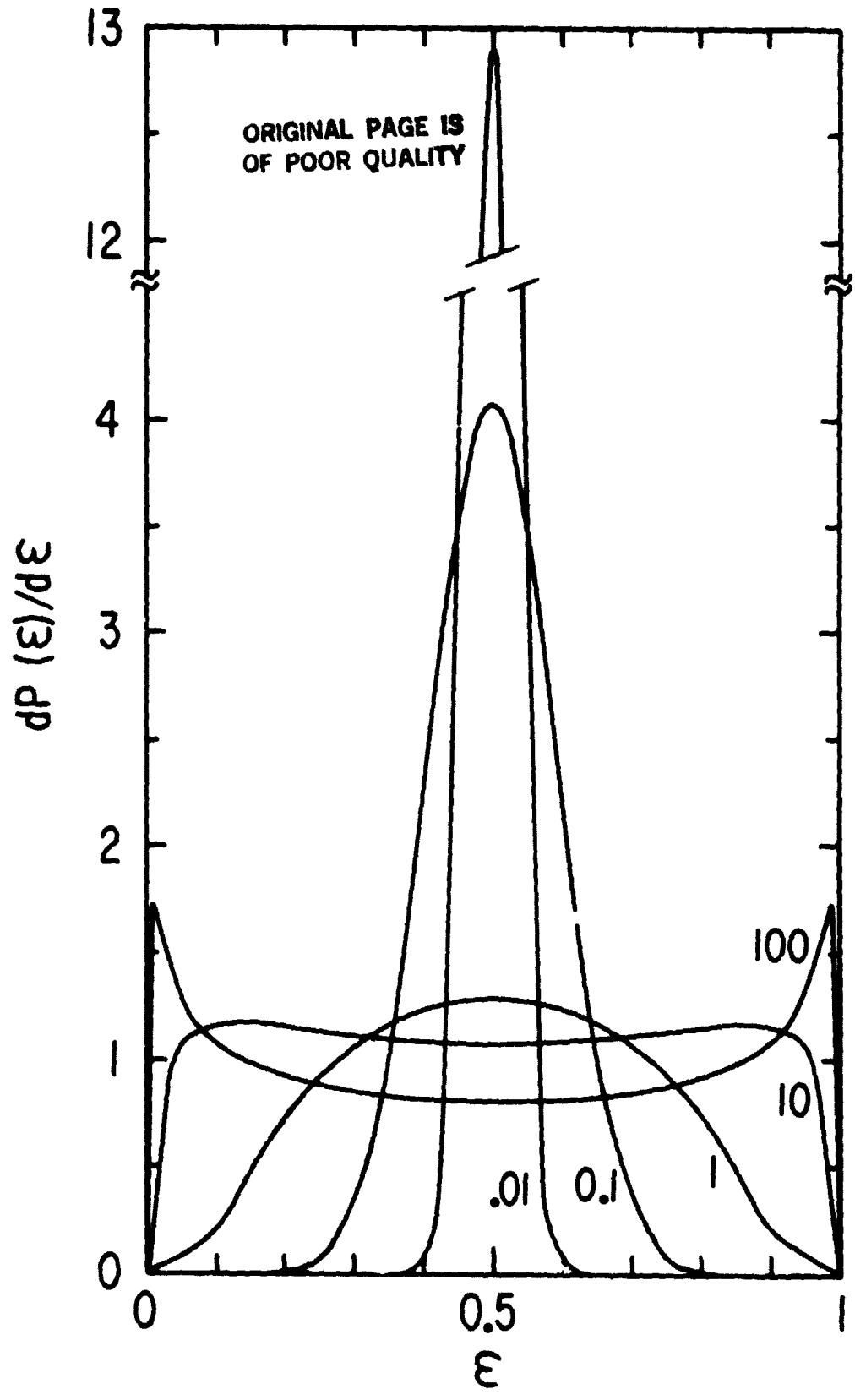
ORIGINAL PAGE IS
OF POOR QUALITY
13
12
4
3
2
1
0
dP (ε)/dε
0
0.5
1
ε
100
10
1
0.1
.01

Figure 7

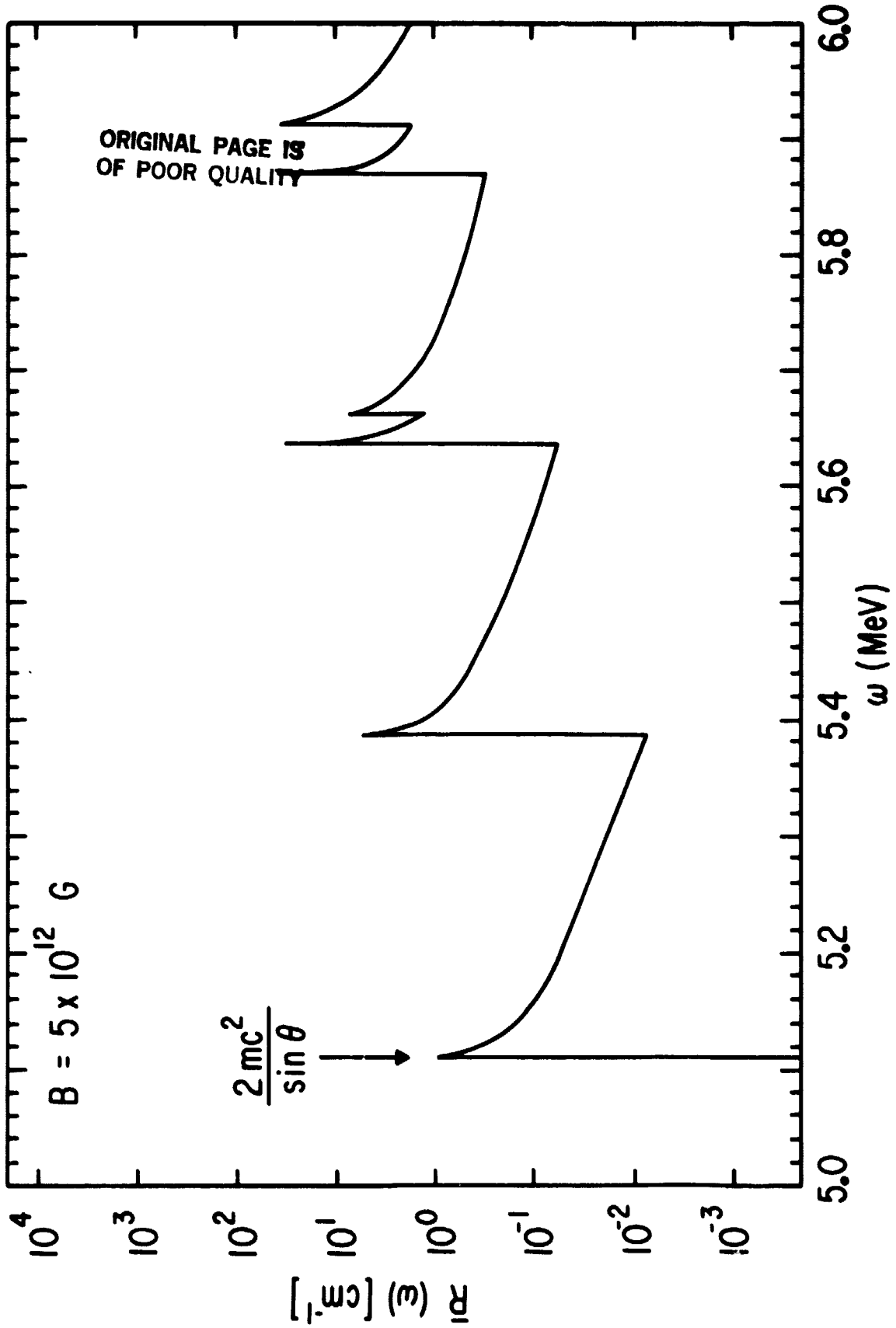
ORIGINAL PAGE IS
OF POOR QUALITY
B = 5 x 10^12 G
2mc^2 / sin θ
R (ω) [cm^-1]
ω (MeV)
10^4
10^3
10^2
10^1
10^0
10^-1
10^-2
10^-3
5.0
5.2
5.4
5.6
5.8
6.0

Figure 8